

VĚDECKÉ SPISY VYSOKÉHO UČENÍ TECHNICKÉHO V BRNĚ

Edice Habilitační a inaugurační spisy, sv. 753

ISSN 1213-418X

Hana Šimonová

**FRACTURE AND FATIGUE PARAMETERS
OF ADVANCED BUILDING MATERIALS
WITH BRITTLE MATRIX**

**BRNO UNIVERSITY OF TECHNOLOGY
FACULTY OF CIVIL ENGINEERING
INSTITUTE OF STRUCTURAL MECHANICS**

Ing. Hana Šimonová, Ph.D.

**FRACTURE AND FATIGUE PARAMETERS OF ADVANCED
BUILDING MATERIALS WITH BRITTLE MATRIX**

**LOMOVÉ A ÚNAVOVÉ PARAMETRY POKROČILÝCH STAVEBNÍCH
MATERIÁLŮ S KŘEHKOU MATRICÍ**

**SHORT VERSION OF HABILITATION THESIS
FIELD: CONSTRUCTIONS AND TRAFFIC STRUCTURES**



BRNO 2023

KEYWORDS

Fracture, fatigue, experiment, quasi-brittle, composite, test configuration, fracture model.

KLÍČOVÁ SLOVA

Lom, únava, experiment, kvazikřehký, kompozit, zkušební konfigurace, lomový model.

DEPOSITARY OF THESIS

The original thesis is stored in the archives of the Office for Internal and External Relations of the Faculty of Civil Engineering, Brno University of Technology, Veveří 331/95, 602 00 Brno, Czech Republic.

© Hana Šimonová, 2023

ISBN 978-80-214-6155-0

ISSN 1213-418X

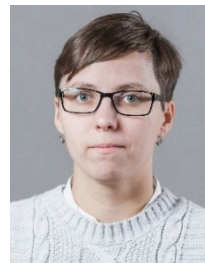
CONTENTS

CURRICULUM VITAE	4
1 INTRODUCTION.....	5
2 MATERIALS UNDER STUDY	5
3 FRACTURE TESTS OF QUASI-BRITTLE MATERIALS	6
3.1 SPECIMENS AND FRACTURE TESTS CONFIGURATIONS	7
3.2 TESTING MACHINES AND DETAILS OF FRACTURE TEST COURSE	9
3.3 ADJUSTMENT OF RECORDED DATA.....	11
3.4 DETERMINATION OF MECHANICAL FRACTURE PARAMETERS	12
4 FATIGUE FRACTURE TESTS	16
4.1 CYCLIC FRACTURE TESTS IN 3PB TEST CONFIGURATION.....	16
4.2 EXPERIMENTAL DETERMINATION OF WÖHLER CURVE	17
4.3 CORRECTION PROCEDURE OF WÖHLER CURVE PARAMETERS	18
5 SUMMARY OF SELECTED RESULTS.....	20
6 CONCLUDING REMARKS	24
REFERENCES.....	25
ABSTRACT.....	32

CURRICULUM VITAE

Personal Information

Name and surname: Hana Šimonová
Date of birth: June 7, 1985
Address: Brno University of Technology (BUT), Faculty of Civil Engineering (FCE), Institute of Structural Mechanics (ISM)
602 00 Brno, Veveri 331/95, Czech Republic
phone: (+420) 541 147 381
e-mail: simonova.h@vutbr.cz
web: <http://www.vutbr.cz/en/people/hana-simonova-81393>



Main Areas of Research

Fracture mechanics and fatigue of quasi-brittle composites field, evaluation of fatigue and static fracture tests of many different types of quasi-brittle materials, from mortars/fine-grained composites (lime with different admixtures such as brick powder, metakaolin, bentonite, metaclay; cement with admixture of slag, fly ash, metakaolin, brick powder; alkali activated slag with admixture of nanotubes, fly ash, shrinkage reducing admixture, cement kiln dust; geopolymer with admixture of nanotubes) to plenty of types of concrete such as plain concrete of different composition (water/cement ratio, with/without superplasticizer), concrete with fibres (different types/length/volume of steel, polymer, natural (e.g. hemp) fibres).

Education

Nov. 2013 **Ph.D.**, BUT, FCE, ISM in the field Constructions and Traffic Structures.
Feb. 2010 **Ing.**, with *honours*, BUT, FCE, ISM in the field Constructions and Traffic Structures.
July 2008 **Bc.**, BUT, FCE, ISM in the field Constructions and Traffic Structures.

Work Experience

Since 07/2019 **Assistant professor** at BUT, FCE, ISM.
01/2019–06/2019 **Researcher and technician for science and research** at BUT, FCE, ISM.
12/2013–12/2018 **Assistant professor** at BUT, FCE, ISM.
03–12/2014 **Technician for science and research** at BUT, FCE, ISM.
02/ 2011–11/2013 **Assistant** at BUT, FCE, ISM.
02–12/2010 **Technician for science and research** at BUT, FCE, ISM.

Research tasks, projects and research fellowship

Principal investigator of the junior research grant project No. 18-12289Y supported by Czech Science Foundation (final evaluation – outstanding project results (of international importance) and the project was among the nominated for the GACR President's awards for 2021) and a member in more than 20 additional research project teams. Principal investigator of 2 projects within the standard specific research program at BUT. Post-doctoral fellowship at Technische Universität Wien (01/2019–06/2019, 09/2014–3/2015).

Publication activities

Author and co-author of over 200 publications, 58 of them indexed in Web of Science database and 96 of them in Scopus database. Number of citations without (all authors)/including self-citations: 162(131)/177 according to Web of Science database and 257(199)/302 according to Scopus database; h-index = 6 in Web of Science database and h-index = 8 in Scopus database.

1 INTRODUCTION

The author of the habilitation thesis was engaged in different research tasks connected with experimental fracture mechanics of quasi-brittle materials within the framework of research projects solved at the Faculty of Civil Engineering, the Brno University of Technology. Therefore, it was decided to create the thesis through a series of published articles which represents an apposite way for the presentation of the obtained results. The main emphasis is put on the experimental determination of mechanical fracture and fatigue characteristics of various types of commonly used but also newly developed building composites with the brittle matrix.

The work is divided into two parts. Part I describes investigated materials, used fracture and fatigue test configurations, processing of experimentally obtained data, and determination of mechanical fracture and fatigue parameters. Part II is constituted through a series of published articles which are divided into five different research topics.

This short version of the habilitation thesis consists of Part I completed by values of mechanical fracture parameters of selected investigated materials with a brittle matrix.

2 MATERIALS UNDER STUDY

Many materials used in civil engineering including concrete as the main representative of this group may be classified as quasi-brittle material, showing the so-called tensile softening, i.e. gradual decrease of transmitting stress in the significant area ahead of the crack/notch tip (fracture process zone FPZ). Studying the mechanical response of specimens made of such composites under static and dynamic/fatigue loading is complicated due to their highly nonlinear nature. Numerical tools for modelling both elastic (elastic-plastic) behaviour and also fracture processes are commonly used to predict or assess this response. Such tools – often based on the finite element method [1] or physical discretization of the continuum [2] – usually exploit a type of nonlinear fracture model that simulates the cohesive nature of the cracking of quasi-brittle material [3–5]. The parameters of this fracture model are determined from records of fracture tests; this is carried out either using evaluation methods built on the principle of the used non-linear fracture model, e.g. the work-of-fracture method [6] or the size effect method [7], or using inverse analysis with the possible application of advanced identification methods [8–10]. The fracture models for quasi-brittle composites are most often based on the standardized geometry of specimens with stress concentrators; the three-point bending test [4] or wedge splitting test [11, 12] are typically used.

Assessment of the fracture behaviour of quasi-brittle materials is usually performed for notched specimens/structures subjected to the mode I of loading. The investigations of the fracture phenomena in other modes of loading and/or their combination (mixed modes of loading) are studied rather rarely even though the real structures made of quasi-brittle materials in civil engineering applications are usually loaded in a mixed-mode manner. It should be also emphasized that many structures are often subjected not only to static but also to repetitive cyclic loads of high-stress amplitude. Examples of such cyclic loads include automotive and train traffic, machine vibration, and wind action. The processes occurring within the quasi-brittle material structure and leading to its degradation under cyclic loading are more complicated in comparison to those affecting metals [13]. That is the reason why knowledge of the behaviour of quasi-brittle materials, not only under static or quasi-static conditions but also under cyclic conditions, is very important for the complex description of crack propagation in such materials. However, fracture and fatigue tests of quasi-brittle materials and structures are expensive and time-consuming, and for this reason, numerical modelling [14, 15] can represent a powerful tool for the prediction of the damage process and fatigue life of such materials under different service conditions. For the effective and correct use of

a numerical (material) model, it is often necessary to tune its parameters using data obtained from experimental measurements. The correct evaluation of such data is becoming a prerequisite for the correct use of numerical models in practice.

Although Portland cement and its blends are and in the near future will be the most common binders in practical applications of civil engineering around the world because of their availability, versatility, and tradition, there are increasing efforts to search for some alternative binders. Nowadays, an important factor in the development of new building materials is their environmental credentials. The rational management of natural resources and the use of waste materials are becoming more and more important [16]. Great emphasis is placed on environmental protection through reductions of CO₂ emissions of which a large amount is produced by cement industries. There are two feasible ways how to reduce the CO₂ emissions in the production of the above-mentioned building materials. The first one is the application of secondary raw materials as supplementary cementitious materials [17]. The other way is using the alkali-activated binder (AAB), this type of material is even more effective in reducing CO₂ emissions and energy consumption [18, 19]. Another option is to reduce raw materials consumption in the concrete mixture by substitution of natural aggregates with recycled aggregates [20–24].

The same as cement-based concrete, materials based on AABs belong to materials with the quasi-brittle response, i.e. low energy absorption capacity under tensile load. Different types of steel or synthetic fibres [25–27] are added to overcome this problem and improve the material's resistance to crack propagation. The environmentally guided trend of research leads to the use of a sustainable alternative to steel and synthetic materials. Naturally available fibres produced from different types of plants (e.g. hemp, flax) grown locally make renewable, biodegradable and relatively cheap alternatives [28, 29].

Knowledge of the mechanical and primarily fracture parameters of composites with a brittle matrix is essential for the quantification of their resistance to crack initiation and growth, as well as for the specification of material model parameters employed for the simulation of the quasi-brittle behaviour of structures or their parts made from this type of composite. Therefore, this work is presented the typical fracture tests and their evaluation using selected fracture models for the characterisation of quasi-brittle materials. Attention was paid to the static and fatigue fracture tests of different types of typical and alternative building materials which were mentioned above.

3 FRACTURE TESTS OF QUASI-BRITTLE MATERIALS

The study of mechanical and primarily fracture properties of existing or newly developed composites with a brittle matrix is essential for the description of their fracture behaviour and quantification of resistance to crack propagation. Nevertheless, in many cases, the attention is still focused on the maximum strength of the material rather than analyzing the properties associated with resistance to crack formation and propagation. The main disadvantages of the fracture tests in context to the characterization using maximum strength values are especially time consumption (one test lasts at least 40 minutes), labour intensiveness, and also the process of evaluation which limits wider utilization in standard practice.

The determination of mechanical fracture parameters is based on standardized fracture experiments on specimens with stress concentrators. The typical fracture test configurations used by the author of this thesis and her colleagues are introduced in this chapter. At first, the type of used specimens and test configurations are introduced. Followed by the description of used testing machines and the details about carrying out fracture tests. A detailed description of experimental data processing and the evaluation of mechanical fracture parameters using selected fracture models are introduced.

3.1 SPECIMENS AND FRACTURE TESTS CONFIGURATIONS

The most commonly used specimen shape for fracture tests is a standardized prism which is typically used for the determination of mechanical characteristics. The prisms with nominal dimensions $40 \times 40 \times 160$ mm and $100 \times 100 \times 400$ mm for composites with fine and coarse aggregate, respectively are usually used. The height of the ligament should be at least 5 times of maximum aggregate size.

The test specimen is provided with a stress concentrator (initial notch) before the test is performed. The central edge notch (Figure 1(a)) with a nominal depth of about 1/3 of the specimen's height is made by a diamond blade saw. The other type of notch shape is the Chevron notch (Figure 1(b)) which is typically used for fracture tests of ceramics, brittle metals or aluminium alloys [30]. The Chevron notch is also used for the determination of fracture parameters of rocks [31]. The core-drilled cylindrical specimens are usually used (Figure 1(c)). The cylindrical specimens can be beneficially used also for the characterization of materials of existing structures [32] when core drilling is used to obtain the material from the structure.

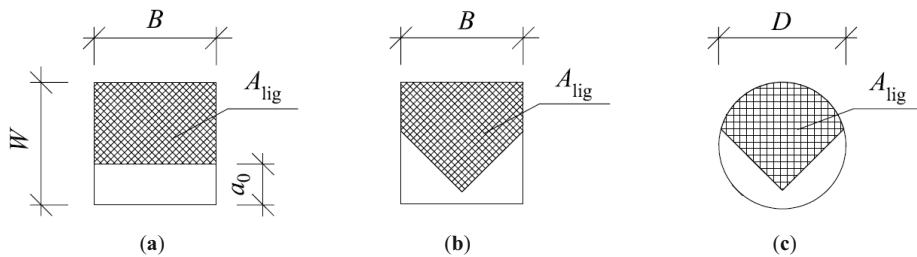


Figure 1. The shape of notch and area of ligament of prismatic/cylindrical test specimens: with edge notch (a), with Chevron notch (b) and (c)

All mentioned test specimens are typically tested in three-point bending (3PB) configuration, see Figure 2(a). The prismatic specimen with a straight-through notch is the most commonly used for the characterization of quasi-brittle materials is 3PB. The main advantages of this configuration are the economy fabrication of both specimen and notch and the relative simplicity of the test procedure. The different types of specimens and notches tested in 3PB were investigated for example in [33].

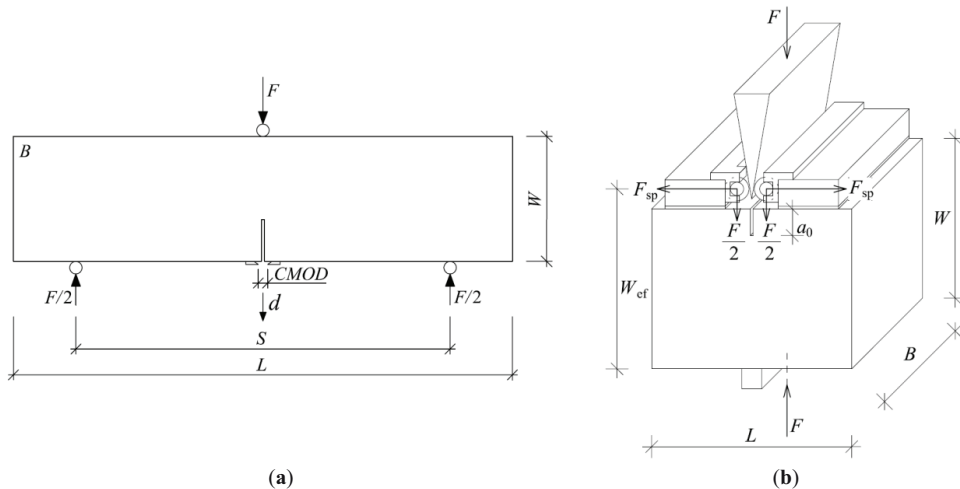


Figure 2. Three-point bending fracture test configuration of a beam specimen with a central edge notch (a); and a wedge-splitting test configuration (b)

The other fracture test configuration used for the characterization of quasi-brittle materials is a wedge-splitting test (WST), see Figure 2(b) [11, 12]. The specimens used for WST are very compact and require a smaller amount of material compared to the 3PB of the prismatic specimen with the straight-through notch. On the other hand, the carrying out of this type of test requires more complicated loading fixtures and the preparation of specimens itself is also much more complicated. For purpose of WST, different types of testing specimens with an initial notch are used. For placing the WST loading fixtures it is necessary to manufacture the rectangular groove on the top of the specimens which is made in different ways. One way is to cut out the groove with a diamond saw which is time-consuming and demanding. The other option is to put a prism with the required dimension of the groove in the mould before the specimens' casting [11]. Figure 3(a) introduced the standardized cubical specimens used for WST with a groove made in one of the above-described ways. The other possibility is to make the groove by glueing two plates on the top of the specimens (Figure 3(b)) [34]. Figure 3(c) introduces the cylindrical specimens which can be used for the characterization of materials drilled from existing structures. The specimens in the WST configuration are placed on one (see Figure 2(b)) or two linear supports. The second case can be found e.g. in [35] in which a detailed experimental campaign of concrete specimens of different sizes tested in 3PB and WST configurations is summarised.

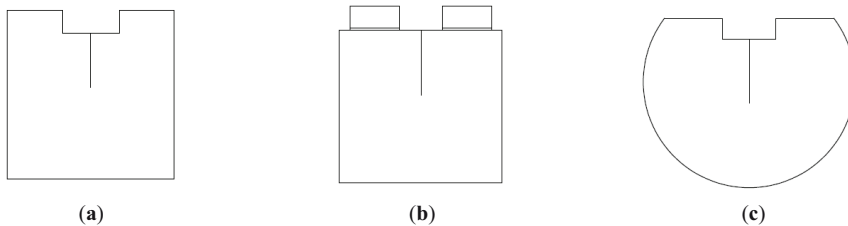


Figure 3. The scheme of test specimens used for WST: cubical specimen with precast or cut-out groove (a), cubical specimen with the groove made by glueing two plates on the top (b), and cylindrical specimen cut-out from the drilled core (c)

The 3PB with the central notch and WST represent the tensile mode I (crack opening) of loading [4, 36]. The investigations of the fracture phenomena in other modes of loading (in-plane shear mode II, out-of-plane shear mode III) and/or their combination (mixed modes of loading) are studied rather rarely even though the real structures made of quasi-brittle materials in civil engineering applications are usually loaded in a mixed-mode manner. For a description of the crack propagation under mixed-mode I/II conditions, various test configurations were used for testing the fracture parameters of rocks and cement-based composites. For this purpose, semi-circular disc specimens in 3PB [37–39], centrally cracked Brazilian disc [39, 40], and prismatic specimens in asymmetric three- [41, 42] or four-point [41, 43] bending configurations are mostly used. Selected semi-circular specimens with an inclined initial notch loaded in 3PB configuration (see Figure 4(a)) were designed for experimental verification of numerical simulations of crack propagation under mixed-mode I/II conditions within the implementation of project “Advanced characterization of cracks propagation in composites based on alkali activated matrix” [44]. The specimens were cast in special silicone moulds with a wooden frame (see Figure 4(b)), which were designed and made by the author of this thesis. The initial notches were made by a water jet cutter. The type of specimens was chosen also concerning the practical application to the in-situ structures when drilled cores are usually taken for verification of real mechanical characteristics from which this type of specimens can be also easily prepared.

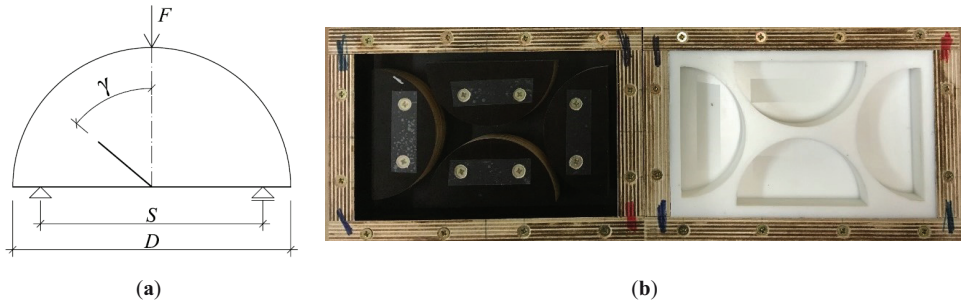


Figure 4. Three-point bending fracture test configuration of a selected semi-circular disc specimen with an inclined initial notch (a); and a special mould (b)

3.2 TESTING MACHINES AND DETAILS OF FRACTURE TEST COURSE

The stiffness of the testing machine is required to be adequate in comparison to the specimen's stiffness to enable stable fracture tests to be conducted without any interruption in the post-peak branch. Several mechanical testing machines which belong to facilities of the laboratories of the Institute of Building Testing FCE BUT are used for conducting the different configurations of fracture tests. In the past, the fracture tests were carried out using a Heckert FPZ 10/1 (Figure 5(a)) or Heckert FPZ 100/1 (Figure 5(b)) testing machines with the different loading range which was set individually according to the strength of tested materials.



Figure 5. The testing machines used for fracture tests: Heckert FPZ 10/1 (a), and Heckert FPZ 100/1 (b)

Nowadays, the stiff multi-purpose mechanical testing machine LabTest 6.250 with a loading range of 0–250 kN (Figure 6(a)) is the most often used or for the larger specimens the LabTest 6-1000.1.10 (Figure 6(b)) with the loading range of 0–1000 kN.

The loading process is in all cases governed by a constant increment of displacement of 0.02 mm/min during the whole course of testing. This loading procedure is slow enough for the whole post-peak behaviour of test specimens to be recorded. The inductive sensor with a measurement range of 0–2 mm is usually used for the measurement of the specimens' deflection in the 3PB configuration. The sensor is mounted into a special frame which is placed on the specimens (Figure 7(a)) or bedded on the upper surface of the specimens during the test (Figure 7(b)). The special frame in Figure 7(a) was designed by the author of this thesis. All frames are constructed to measure the deflection of twofold values in the middle of the span length.

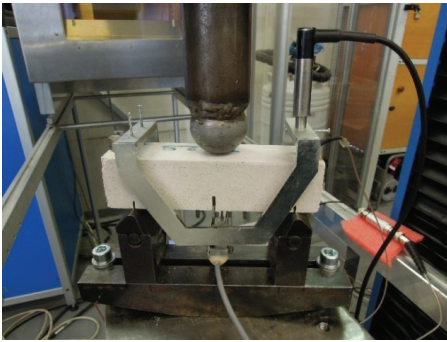


(a)

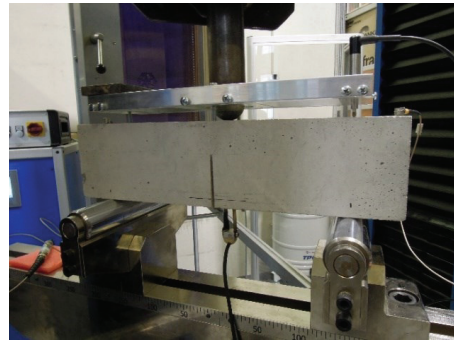


(b)

Figure 6. The testing machines used for fracture tests: LabTest 6.250 (a), and LabTest 6-1000.1.10 (b)



(a)

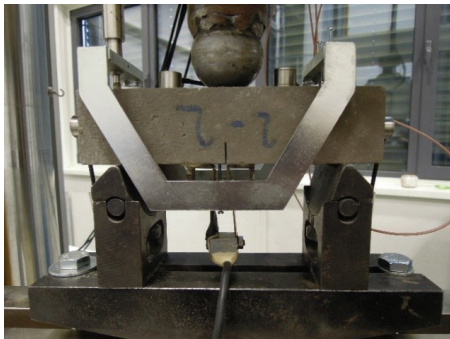


(b)

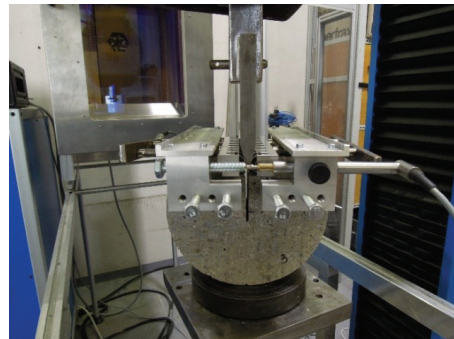
Figure 7. Detail of the test measuring frame: placed on specimen (a), bedded on the upper surface of specimen (b)

The strain gauge is used for the measurement of the crack mouth opening displacement ($CMOD$) in 3PB. It is mounted between two blades glued on the bottom surface of the specimens near the artificial notch ((Figure 8(a)). In the case of WST, the $CMOD$ is measured using pairs of inductive sensors mounted in the special frame (Figure 8(b)).

The mentioned parameters together with loading force and time are continuously recorded by an HBM SPIDER 8 device or HBM Quantum X data-take with the frequency of 5 Hz.



(a)



(b)

Figure 8. Detail of measuring the $CMOD$: 3PB test configuration (a), WST (b)

The advantage of the currently used testing machines is that a 2D video extensometer can be simultaneously used during the fracture test. During the loading process, the strains on the surfaces of the tested specimens are digitally measured using the system with one or two high-frequency cameras, see the example in Figure 9. This measurement system enables monitoring of the real-time crack development and provides high-quality images for further processing using e.g. digital image correlation (DIC). Obtained data could be later used for the analysis of the initiation and development of the FPZ or contactless measurement of deflection and/or $CMOD$ if it is not possible to measure them directly.

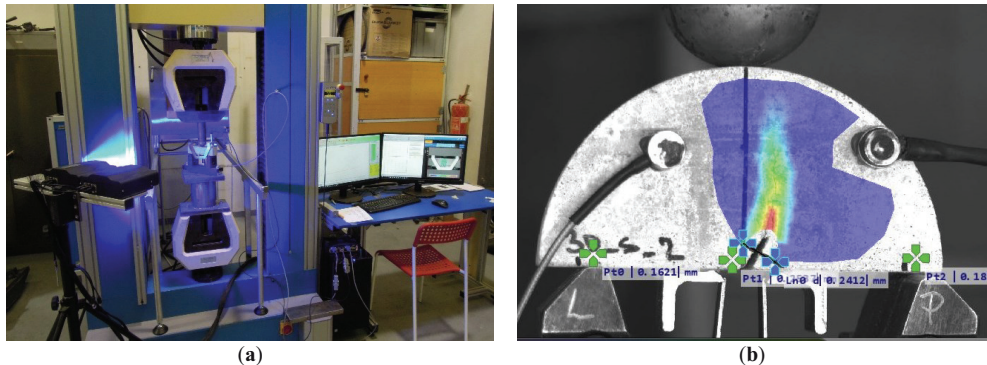


Figure 9. Arrangement of 2D video extensometer measurement (a), and example of crack propagation and measured surface strains (b) in selected 3PB test configurations

3.3 ADJUSTMENT OF RECORDED DATA

The outcome of each fracture test in 3PB configuration is a vertical force F vs. d diagram and F vs. $CMOD$ diagram. The diagrams recorded during the tests are necessary to be processed to obtain the correct input values for consecutive diagram evaluations using the selected fracture models described below.

At the beginning of the specimen loading, small-sized deviations in the measured values of monitored parameters are often recorded. This effect is caused by small unevenness on the specimens' surface being crushed due to the pressure at the support and loading points. These phenomena usually occur over a short period at the beginning of the test, after which the recorded diagram proceeds with a linear part. It follows that it is appropriate to adjust the beginning part of the diagram to obtain the correct input values for the subsequent diagram evaluation. The adjustment of the recorded diagrams is performed in GTDiPS software [45], which is based on advanced transformation methods used for the processing of extensive point sequences. The processing of recorded data is described for the case of $F-d$ diagram for illustration.

Figure 10(a) shows the recorded data from the fracture test. The loading during the fracture test is compressive and because of the setting of the testing machine, the recorded values of load are negative. As above-mentioned, the measured deflection is a twofold value of the midspan deflection which is necessary to know for further $F-d$ diagram evaluation. Therefore, the first step of recorded data adjustment consists of the change of the minus sign of recorded load values, the division of recorded deflection by two, and the elimination of duplicate points (Figure 10(b)).

The second step is shifting the origin of the coordinate system which consists of the removal of the initial part of the diagram ending at the point where is the maximum derivative, the approximation of the beginning part of the diagram by a straight line which is used to find

the point of intersection with a horizontal axis, and the shifting of all points of the diagram equidistantly, thus making the point of intersection the new origin of the coordinate system (Figure 10(c)).

Figure 10(d) shows the final $F-d$ diagram which is used for further determination of mechanical fracture parameters. The last step of adjustments consists of the smoothing of the diagram and the reduction of the number of points.

It is worth noticing that the same procedure is applied also to processing the recorded $F-CMOD$ diagrams from 3PB tests and of course also to the other types of fracture test configurations.

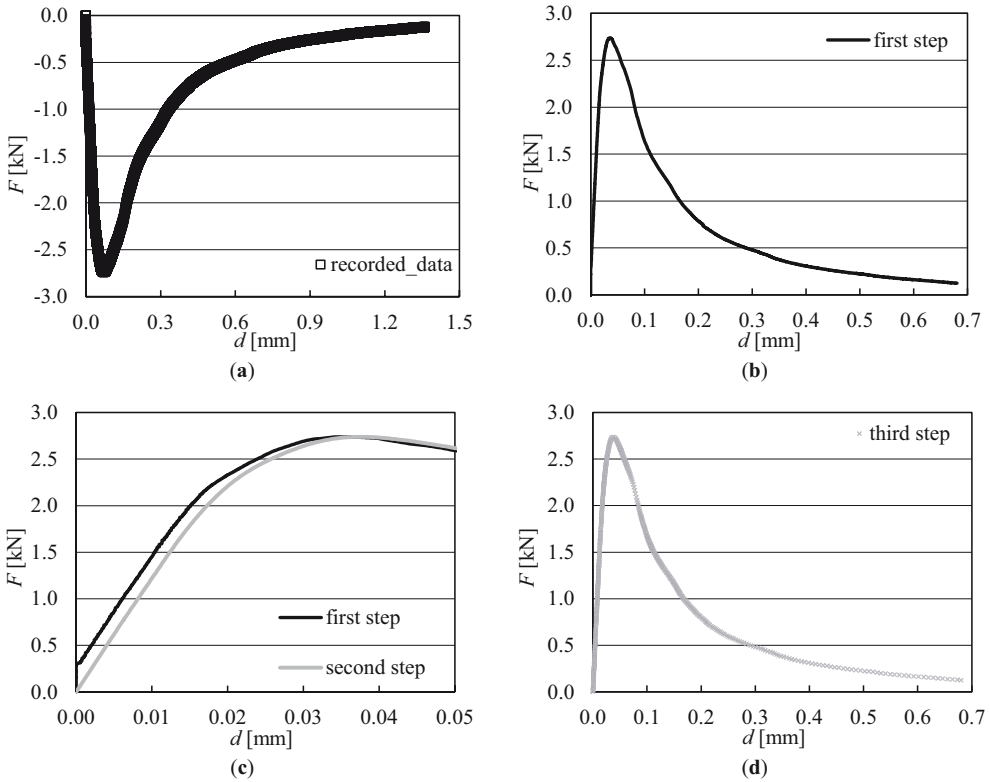


Figure 10. Detail of processing of $F-d$ diagram: recorded data (a), data after the first step of adjustment (b), data after the second step of adjustment – detail of diagram until peak load (c), and data after the third step of adjustment – final diagram used for further evaluation (d)

3.4 DETERMINATION OF MECHANICAL FRACTURE PARAMETERS

As above-mentioned, the most commonly used fracture test configuration is 3PB of the prismatic specimen with the edge notch. Therefore, the determination of mechanical fracture parameters from records of this type of test using the selected fracture models is described in this section.

The value of the static modulus of elasticity E is calculated from the initial part of the $F-d$ diagrams according to [4] with modification by Stibor [46]:

$$E = \frac{F_i}{4Bd_i} \left(\frac{S}{W} \right)^3 \left[1 - 0.387 \frac{W}{S} + 12.13 \left(\frac{W}{S} \right)^{2.5} \right] + \frac{9}{2} \frac{F_i}{Bd_i} \left(\frac{S}{W} \right)^2 F_1(\alpha_0), \quad (1)$$

where F_i is the vertical force in the ascending linear part of the diagram, B is the specimen width, d_i is the midspan deflection corresponding to the force F_i , W is the specimen height, S is the span length (see Figure 2(a)), and

$$F_1(\alpha_0) = \int_0^{\alpha_0} \alpha Y^2(\alpha) d\alpha, \quad (2)$$

where $\alpha = a/W$ is relative crack length and then $\alpha_0 = a_0/W$ is relative notch depth (a_0 is the initial notch depth), and $Y(\alpha)$ is the geometry function for the 3PB configuration proposed by Brown and Strawley [4]:

$$Y(\alpha) = 1.93 - 3.07\alpha + 14.53\alpha^2 - 25.11\alpha^3 + 25.80\alpha^4. \quad (3)$$

The fracture toughness value is determined based on the linear elastic fracture mechanics (LEFM) approach for brittle fracture. This parameter is related to the stress field near the tip of the crack. The fracture toughness value K_{Ic} is calculated using this formula [4]:

$$K_{Ic} = \frac{6M_{\max}}{BW^2} Y(\alpha_0) \sqrt{a_0}, \quad (4)$$

where M_{\max} is the bending moment due to the maximum load F_{\max} and self-weight.

Several adaptations of LEFM have been proposed to cover the nonlinear behaviour of the quasi-brittle materials. One of them is the effective crack model ECM [4], which includes the effect of the pre-peak nonlinear behaviour of a real quasi-brittle structure containing the initial notch through an equivalent elastic structure containing a notch of effective length $a_e > a_0$. The effective crack length a_e is calculated from the secant stiffness of the specimen corresponding to the maximum load F_{\max} and matching midspan deflection $d_{F_{\max}}$. The a_e for the prismatic specimen with a central edge notch tested in the 3PB configuration is determined according to [4] from the following relationship:

$$d_{F_{\max}} = \frac{F_{\max}}{4BE'} \left(\frac{S}{W}\right)^3 \left[1 + \frac{5qS}{8F_{\max}} + \left(\frac{W}{S}\right)^2 \left\{ 2.70 + 1.35 \frac{qS}{F_{\max}} \right\} - 0.84 \left(\frac{W}{S}\right)^3 \right] + \frac{9}{2} \frac{F_{\max}}{BE'} \left(1 + \frac{qS}{2F_{\max}}\right) \left(\frac{S}{W}\right)^2 F_1(\alpha_e), \quad (5)$$

where E' is the static modulus of elasticity corresponding to secant stiffness, and q is the self-weight of the specimens per unit length.

Subsequently, the effective fracture toughness value K_{Ice} is calculated using a LEFM formula eq. (4) where α_0 is replaced by α_e . Since the effective crack length a_e is in eq. (2) as the argument of integral, the problem is solved by an iterative method.

The complete $F-d$ diagrams, including their post-peak parts, are employed to determine the work of fracture W_F value, which is given by the area under the diagram. In this case, W_F is calculated according to the Stibor [46], where the area under the measured diagram, the effect of the unmeasured part, and the self-weight of the specimen are considered. After that, the specific fracture energy G_F value is determined according to the RILEM recommendation [6] as the average energy given by dividing the total W_F by the projected fracture area A_{lig} (i.e. the area of the initially uncracked ligament):

$$G_F = \frac{W_F}{(W - a_0)B}. \quad (6)$$

The double- K fracture (2 K) model [47] is used for the evaluation of the $F-CMOD$ diagrams to determine selected fracture parameters. The parameters describing different phases of the fracture process are determined using this fracture model. The unstable fracture toughness K_{Ic}^{um} is defined as

the critical stress intensity factor corresponding to the F_{\max} and it represents the phase of unstable crack propagation. This parameter is similar to the effective fracture toughness K_{Ic} used in the ECM by Karihaloo [4]. The equivalent elastic crack length a_c is determined from the following equation [47]:

$$CMOD_{F_{\max}} = \frac{6F_{\max}Sa_c}{BW^2E}V(\alpha'_c), \quad (7)$$

where $CMOD_{F_{\max}}$ is $CMOD$ corresponding to maximum load F_{\max} , and

$$V(\alpha'_c) = 0.76 - 2.28\alpha'_c + 3.87\alpha'_c{}^2 - 2.04\alpha'_c{}^3 + \frac{0.66}{(1 - \alpha'_c)^2}, \quad (8)$$

where $\alpha'_c = (a_c + H_0) / W + H_0$; H_0 is the thickness of blades fixed on the bottom surface of the specimens between which the strain gauge is placed.

Once the equivalent elastic crack length a_c is known, the K_{Ic}^{un} is determined according to eq. (4) where α is replaced with α_c , and the geometry function is in this case [4]:

$$Y(\alpha_c) = \frac{1.99 - \alpha_c(1 - \alpha_c)(2.15 - 3.93\alpha_c + 2.70(\alpha_c)^2)}{(1 + 2\alpha_c)(1 - \alpha_c)^{3/2}}. \quad (9)$$

The important parameter for the nonlinear fracture mechanics calculations is the relation between the stress and crack opening displacement, see Figure 11.

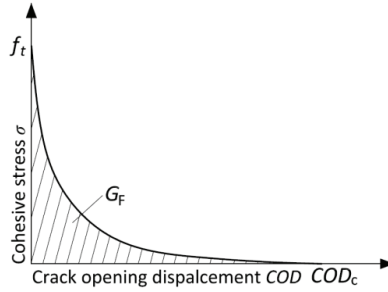


Figure 11. The parameters of softening function

The fracture energy G_F is a derivative parameter of this relation, which represents the area under this curve (softening function). There are two ways how to obtain the parameters of the softening function. The first way is based on the experimental determination of the G_F from the uniaxial tensile strength test with deformation-controlled loading. The G_F is then calculated as the area under the σ - COD diagram. However, it is quite complicated to perform such a test in a stable way for the specimen made of quasi-brittle material, i.e. to catch also the post-peak part of the diagram. Another way consists of the indirect method of determination of critical crack opening displacement COD_c . In this case, the G_F , tensile strength f_t , determined experimentally from the 3PB test and uniaxial tensile test, respectively, and the suitable shape of softening function are the input parameters [48]. Based on the author's previous studies it can be stated that the type of softening function (bilinear or nonlinear) had no significant effect on the calculated values of fracture parameters. The input parameters of the softening function are more important, especially the way of estimation of tensile strength. As above-mentioned, carrying out the uniaxial tensile test for quasi-brittle materials is quite complicated. Therefore, the compressive strength values are commonly used for the estimation of the tensile strength of the materials. However, it is more appropriate to determine the tensile strength by an inverse analysis, for example, based on the artificial neural network [49, 50]. The principle consists in the identification of the material parameters, which gives the corresponding

F - d diagrams response as obtained during real-time specimen loading. It is presumed that such strength is very close to the uniaxial tensile strength.

In the 2K model, the softening function has to be also known to calculate cohesive toughness at critical condition K_{Ic}^c , which can be interpreted as an increase in the resistance to crack propagation caused by bridging of aggregate grains and other toughening mechanisms in the fracture process zone FPZ [47]. In the following part, the relations using the nonlinear softening function according to Hordijk [48] are introduced for illustration. The cohesive stress $\sigma(CTOD_c)$ at the tip of an initial notch at the critical state can be then obtained from this softening function:

$$\sigma(CTOD_c) = f_t \left\{ \left[1 + \left(c_1 \frac{CTOD_c}{COD_c} \right)^3 \right] \exp\left(-c_2 \frac{CTOD_c}{COD_c}\right) - \frac{CTOD_c}{COD_c} (1 + c_1^3) \exp(-c_2) \right\}, \quad (10)$$

where $CTOD_c$ is the critical crack tip opening displacement according to Jenq and Shah [51]:

$$CTOD_c = CMOD_{F_{max}} \left(\left(1 - \frac{a_0}{a_c} \right)^2 + (1.081 - 1.149\alpha_c) \left(\frac{a_0}{a_c} - \left(\frac{a_0}{a_c} \right)^2 \right) \right)^{1/2}, \quad (11)$$

and c_1 and c_2 are the material constants, which are taken from [47]. COD_c is calculated using the value of fracture energy G_F determined using eq. (6) or by the inverse analysis [49, 50] according to this formula:

$$COD_c = \frac{5.136G_F}{f_t}. \quad (12)$$

Subsequently, the linear function for the calculation of cohesive stress $\sigma(x)$ along the length of the equivalent elastic crack can be formulated:

$$\sigma(x) = \sigma(CTOD_c) + \frac{x - a_0}{a_c - a_0} (f_t - \sigma(CTOD_c)). \quad (13)$$

Once this relation is known, the cohesive fracture toughness K_{Ic}^c is determined as follows:

$$K_{Ic}^c = \int_{a_0/a_c}^1 2 \sqrt{\frac{a_c}{\pi}} \sigma(U) F(U, \alpha_c) dU, \quad (14)$$

where the substitution $U = x/a_c$ is used and $F(U, \alpha_c)$ is determined according to [52]:

$$F(U, \alpha_c) = \frac{3.52(1-U)}{(1-\alpha_c)^{3/2}} - \frac{4.35-5.28U}{(1-\alpha_c)^{1/2}} + \left(\frac{1.30-0.30U^{3/2}}{(1-U^2)^{1/2}} + 0.83 - 1.76U \right) [1 - (1-U)\alpha_c]. \quad (15)$$

The following formula based on the formerly obtained parameters is used to calculate the initial cracking toughness K_{Ic}^{ini} :

$$K_{Ic}^{ini} = K_{Ic}^{un} - K_{Ic}^c, \quad (16)$$

the K_{Ic}^{ini} represents the beginning of stable crack propagation.

At last, the load level F_{ini} , which expresses the load at the outset of stable crack propagation from the initial notch, is determined according to the relation:

$$F_{ini} = \frac{4 \cdot S_M \cdot K_{Ic}^{ini}}{S \cdot Y(\alpha_0) \cdot \sqrt{a_0}}, \quad (17)$$

where S_M is the section modulus (calculated as $S_M = 1/6 \cdot B \cdot W^2$), and $Y(\alpha_0)$ is the geometry function according to eq. (9) where α_0 is used instead of α_c .

4 FATIGUE FRACTURE TESTS

Many structures in civil engineering are often subjected not only to static but also to repetitive cyclic loads of high-stress amplitude. The phenomenon known as material fatigue, a process in which progressive and permanent internal damage occurs in materials subjected to repeated loading, is a serious problem also for quasi-brittle materials [13]. The processes are connected with the progressive growth of internal microcracks which on a macro level leads to changes in material properties. Therefore, for the complex description of damage processes in quasi-brittle materials is knowledge of fatigue behaviour very important.

Concrete and other quasi-brittle materials are highly heterogeneous materials and thus processes occurring within their structure and leading to their degradation under cyclic loading are more complicated in comparison to those affecting metals [13]. This is one reason why the understanding of fatigue failure in these materials is still lacking in comparison to that of ferrous materials, even though concrete is a widely used construction material.

As in the case of static tests, different loading arrangements have been used in fatigue testing, including compression [53], tension [54], and bending [55, 56] tests. The most common method of fatigue testing, by far, is using the bending tests, also the test specimens with an initial stress concentrator are used [57, 58].

As in the case of static fracture tests, the author's attention is paid to the evaluation of the cyclic 3PB test and the determining fatigue characteristics of composites with the brittle matrix. The cyclic tests are much more time-consuming compared to static ones. Therefore, to achieve a relevant evaluation of experiments, it is necessary in the case of quasi-brittle materials to consider also the ageing of specimens. A correction procedure of the measured data based on static compressive strength measurements covering the time interval of performing the fatigue tests was suggested and checked. The procedure is applied to Wöhler curves obtained from cyclic 3PB tests of beam specimens with a central edge notch.

4.1 CYCLIC FRACTURE TESTS IN 3PB TEST CONFIGURATION

The most commonly used specimen shape for cyclic tests is also a standardized prism which is typically used for the determination of mechanical characteristics. The prisms with nominal dimensions $40 \times 40 \times 160$ mm and $100 \times 100 \times 400$ mm for composites with fine and coarse aggregate, respectively are usually used. The specimens are before testing provided with the central edge notch (see ligament in Figure 1(a)) with a nominal depth of about 1/10 of the specimen's height which is made by a diamond blade saw.

The fatigue experiments are typically carried out using servo-hydraulic testing machines. Figure 12(a) introduces an example of such a testing machine the Zwick/Roell Amsler HC25 with a loading range of 0–25 kN, which belongs to laboratories of the Institute of Physics of Materials (IPM), Czech Academy of Sciences (CAS). The author of this thesis cooperates with colleagues from IPM, CAS in conducting and evaluating fatigue tests of specimens made of different quasi-brittle materials over a long period. The typical arrangement of a 3PB cyclic fracture test configuration is shown in Figure 12(b).

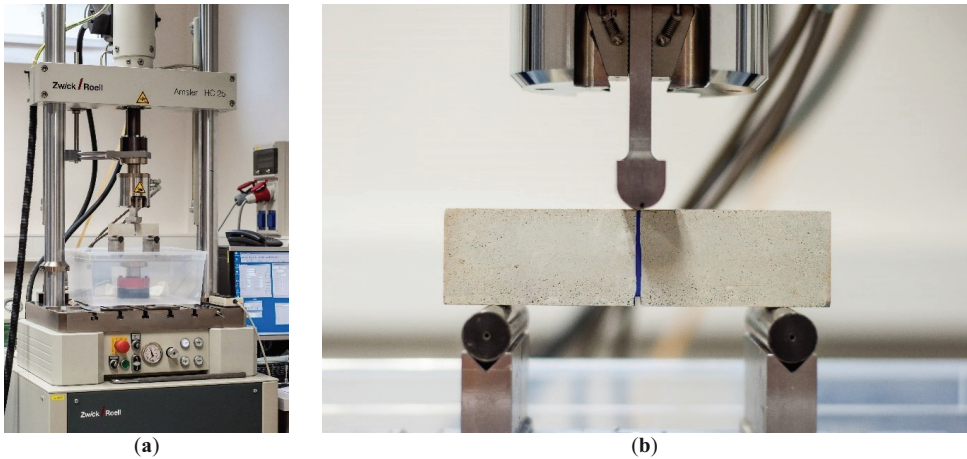


Figure 12. The testing machine used for cyclic/fatigue fracture test (a), the arrangement of cyclic test in 3PB configuration (b)

In practice, the structures are subjected to random fatigue loading. This process of loading is very difficult to model in laboratory conditions, therefore there is an effort to simplify the course of loading. The most frequent way is the replacement of the random loading by sinusoidal load, which is also used in experiments described here. The cyclic loading process is governed by a force; the force amplitude is controlled. The stress ratio $R = F_{F\min}/F_{F\max} = 0.1$, where $F_{F\min}$ and $F_{F\max}$ refer to the minimum and maximum load of a sinusoidal wave in each cycle. The load frequency is set to 10 Hz to cover all fatigue regions in a reasonable time. The number of cycles N at failure is recorded for each specimen.

The fatigue loading is traditionally divided into two categories [59] i.e. low-cycle and high-cycle loading. Low-cycle loading involves the application of a few load cycles at high-stress levels. On the other hand, high-cycle loading is characterized by a large number of cycles at lower stress levels. In this chapter, attention is paid to high-cycle fatigue. Therefore, the upper limit to the number of cycles N to be applied is selected as 2 million cycles. The test is finished when the failure of the specimen occurred or the upper limit of loading cycles is reached, whichever occurred first.

4.2 EXPERIMENTAL DETERMINATION OF WÖHLER CURVE

Various approaches have been used to assess the fatigue life of structural members in recent years. The generally accepted approach in engineering practice is based on empirically derived S_F-N diagrams known as Wöhler curves (applied stress during the load cycle S_F vs. the number of cycles to failure N), see Figure 13. S_F-N test data are usually displayed in a semi-logarithmic plot, where its course is approximated by slanting and horizontal lines. The parameters of the S_F-N curve are determined only for test specimens that are broken during the cyclic test (circles in Figure 13), the specimens which withstand 2 million cycles are not taken into consideration (run-outs – circles with arrows in Figure 13). With respect to the time demand of cyclic tests, the fatigue limit is determined as the highest stress level at which three test specimens withstand 2 million cycles. However, this fatigue limit is not finite, and fatigue failure can occur with more load cycles.

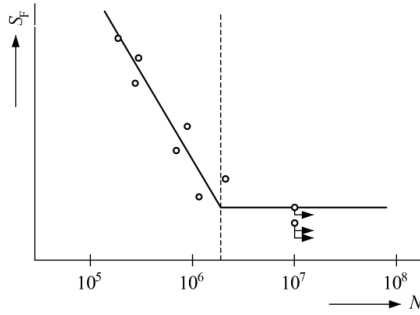


Figure 13. Typical S_F - N (Wöhler) curve according to [60]

The S_F - N curve can be constructed covering different stress levels depending on the used load for its determination, i.e. using the maximum load of a sinusoidal wave F_{Fmax} , the load amplitude $F_a = (F_{Fmax} - F_{Fmin}) / 2$ or the load range $\Delta F = F_{Fmax} - F_{Fmin}$.

Fatigue tests of quasi-brittle materials are characterized by a relatively large scattering of the measured number of cycles at individual stress levels, therefore for an appropriate determination of the Wöhler curve, several specimens have to be tested at each stress level. The first stress level is equal to effective flexural strength. Then stress level is reduced gradually by approximately 10 % and the specimen is loaded with cyclic load until its failure or when the fatigue limit is reached. A minimum of 8–12 specimens of tested material is necessary to determine the Wöhler curve. For a more accurate determination of its parameters or its statistical evaluation, 15–20 specimens are needed.

There are several mathematical descriptions of the Wöhler curve, one of them is Basquin's power law [61]:

$$S_F = a \cdot N^b \quad (18)$$

where a and b are material constants.

4.3 CORRECTION PROCEDURE OF WÖHLER CURVE PARAMETERS

Theoretically, all test specimens are broken after the same number of cycles for one particular stress level. However, the fatigue behaviour of heterogeneous quasi-brittle materials is distant from an optimal case and the results show variability. On that account, it is necessary to determine not only the analytical expression of the corresponding S_F - N curve but also the close-fitting of regression, such as the coefficient of determination R^2 . The variability is connected also with the time demand of cyclic tests which leads to the different ages and thus materials characteristics of the individual specimen during the cyclic tests. The suggested correction procedure allows a more accurate determination of the fatigue parameters corresponding to the age of the specimen when the cyclic test is performed.

The measured stress levels of the S_F - N curve are divided by coefficients determined from the approximation curve of relative compressive strength values to obtain correct values of fatigue characteristics corresponding to the age of the specimen at which a particular cyclic test is performed. The measured data are standardized to a particular age of specimens by this procedure. Compressive strength is chosen because it is the most commonly determined mechanical parameter of quasi-brittle composites and it is used as an input parameter in the structural design. The compressive strength test is also less time-consuming in comparison with the static fracture test.

Nevertheless, the presented procedure can be used with any other mechanical or fracture parameter [62].

The measured values of compressive strength are divided by the average value at the chosen specimen's age. In the example presented below in Figure 14, the compressive strength values at the specimen's age of 28 days are chosen. The compressive strength at the age of 28 days is usually used as a reference value in the design of cement-based composites. However, in the case of composites based on alkali-activated binder (AAB) the mechanical fracture parameters significantly changes during the specimen's ageing also after 90 days so different reference age of specimens can be chosen based on the investigated material. By this procedure, the relative compressive strength values for all investigated ages of specimens are obtained. These values are then approximated by the selected function. The modified form of the function according to Abdel-Jawad [63] is presented here:

$$rf_c = c \cdot (1 - e^{-m \cdot t^n}) \quad (19)$$

where t is the specimen's age in days, rf_c is the dimensionless relative compressive strength, c is the coefficient corresponding with an asymptote of the approximation curve, in other words, the ratio of the theoretical value of the compressive strength at Infinitum to the value of compressive strength at the chosen specimen's age, and m , n are the coefficients corresponding with the size of the time-dependent change of compressive strength, which is generally dependent on the compositions of the used mixture. The approximation is performed using the GTDiPS software [45]. The procedure is based on the nonlinear least-square method provided by genetic algorithms which are implemented in this open-source Java GA package [45].

The above-described procedure can be applied also by using simple approximation (regression) curves which cover only the interval in which fatigue tests are performed [62]. For example, the power, logarithmic or polynomial trendline is possible to use, which is part of MS EXCEL software.

For illustration, the approximation curve and its coefficients according to eq. (19) for relative compressive strength values related to the mean value of this parameter at the specimen's age of 28 days of C30/37 strength class concrete is displayed in Figure 14(a). In this case, the cyclic tests of concrete specimens were performed between the age of 30 to 150 days. From Figure 14(a) is evident that the compressive strength value increased in this interval by about 25 %. The results of cyclic fracture tests of specimens in 3PB configuration at different load levels are summarized in Figure 14(b) in the form of the Wöhler curve (eq. (18)). The coefficient of determination R^2 of the S_F-N curve determined directly from the measured values is relatively low for this type of concrete. In addition to the measured data, the standardized data using the coefficients obtained from the advanced approximation curve of the relative compressive strength values (Figure 14(a)) are also plotted, including the analytical expression of the S_F-N and R^2 . This procedure led to a significant increase in the value of the dimensionless coefficient of determination R^2 from 0.38 to 0.70. The obtained results can be considered as evidence of the efficacy of the described correction procedure.

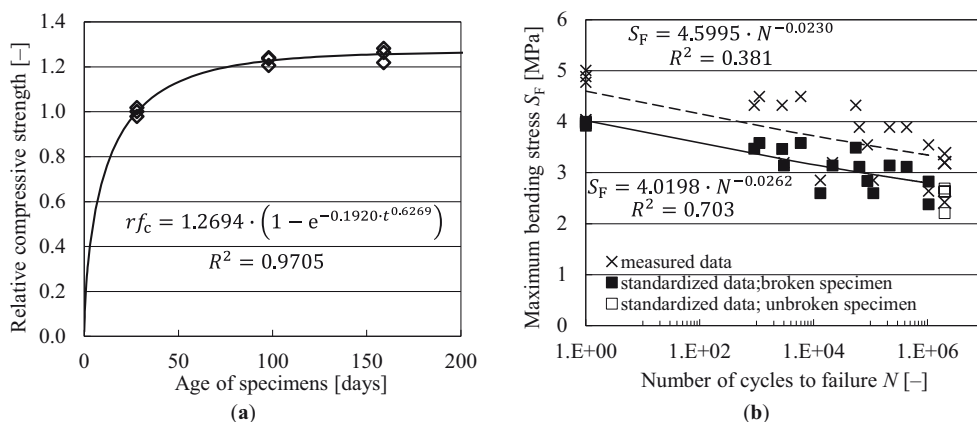


Figure 14. The approximation curve for relative compressive strength values related to the specimen's age of 28 days (a), the example of S_F - N curve plotted for measured and standardized data at the specimen's age of 28 days; the horizontal axis is plotted in logarithmic scale (b)

5 SUMMARY OF SELECTED RESULTS

The compressive strength vs. effective fracture toughness or specific fracture energy is plotted in the following Figures for illustration of different behaviour of selected previously mentioned investigated materials and to indicate the extensiveness of the evaluated fracture tests. Because of better readability, the wide range of investigated materials was divided into three groups:

- Figures 15, 16: fine-grained composites based on different matrixes: AAS – alkali-activated slag, AABP – alkali-activated brick powder, GFA – fly ash based geopolymer, C – cement; C_modified – cement modified with different admixtures; L_modified – lime modified with different admixtures. The specimens with nominal dimensions of $40 \times 40 \times 160$ mm were used.
- Figures 17, 18: fine-grained composites based on different alkali-activated matrixes (AAS, GFA, GMK – metakaolin based geopolymer) with different reinforcement: SF – steel microfibres, HF – hemp fibres, CNT – carbon nanotubes, MIX – a combination of glass and flax fibres. The specimens with nominal dimensions of $40 \times 40 \times 160$ mm were used.
- Figures 19, 20: concrete mixtures with coarse aggregate with different strength classes and temperature loading. The specimens with nominal dimensions of $100 \times 100 \times 400$ mm were used.

The one point in the graph represents the mean value (determined at least from three specimens) of individual parameter for composite with a particular composition. The error bars represent the sample standard deviations.

The detailed results of the mechanical fracture behaviour of individual investigated materials and their compositions could be found in the cited references and also in Part II of the full version of the habilitation thesis.

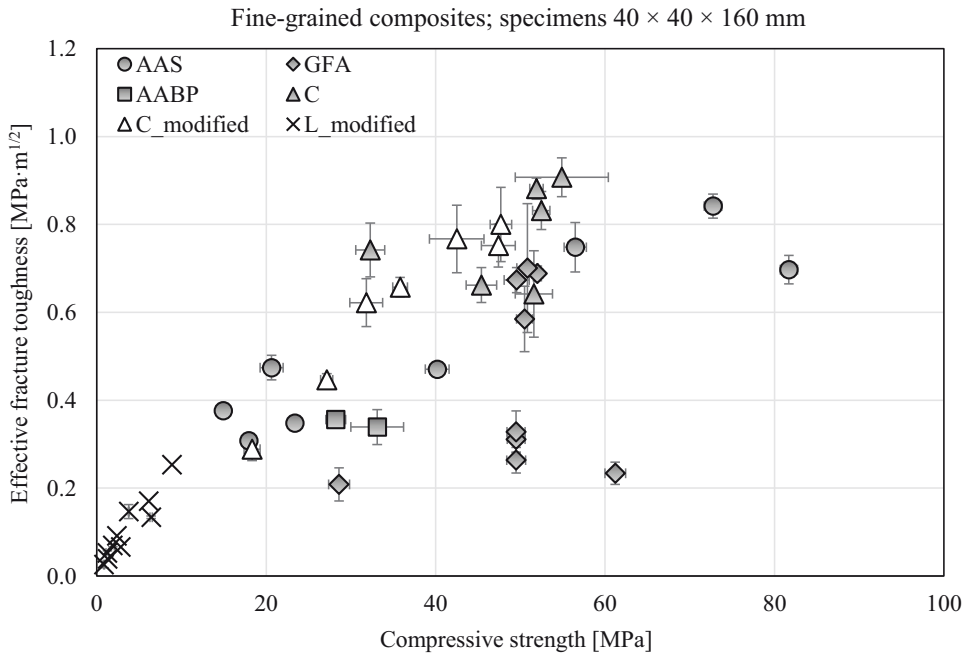


Figure 15. The effective fracture toughness vs. compressive strength of selected investigated fine-grained composites of different compositions

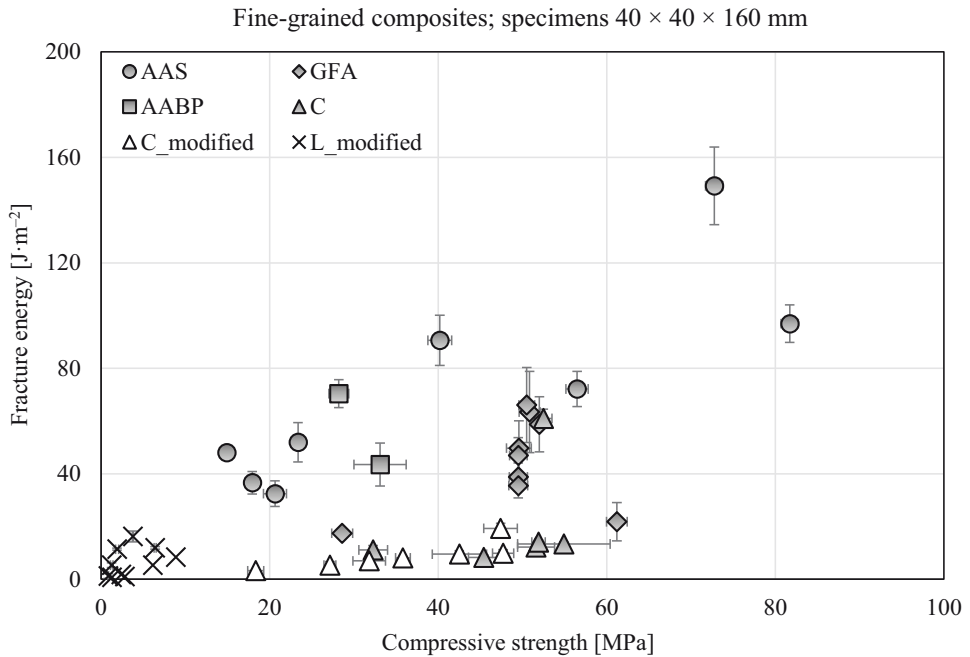


Figure 16. The specific fracture energy vs. compressive strength of selected investigated fine-grained composites of different compositions

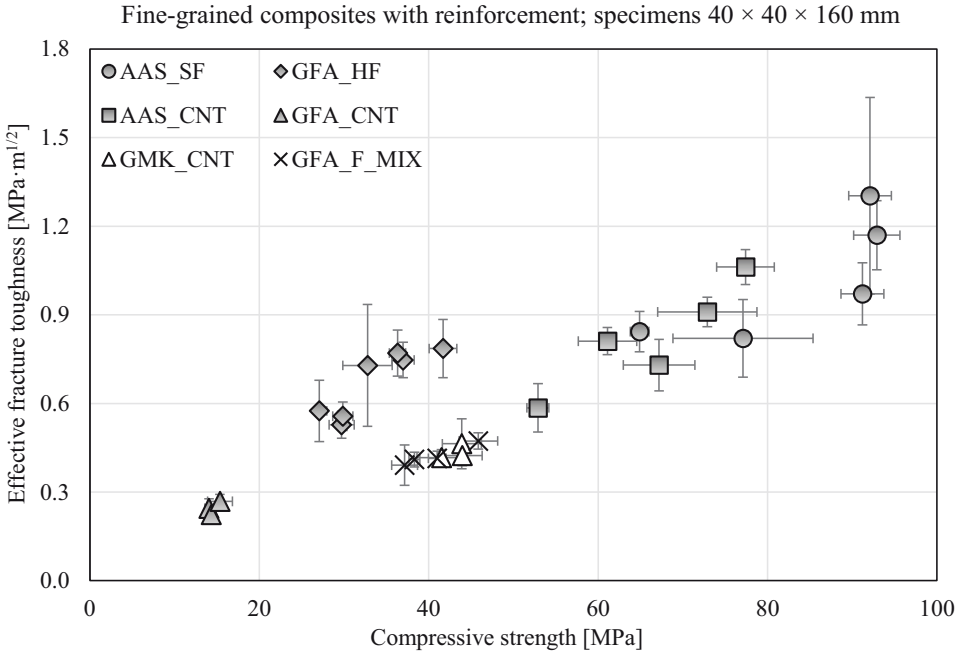


Figure 17. The effective fracture toughness vs. compressive strength of selected investigated fine-grained composites with different reinforcement

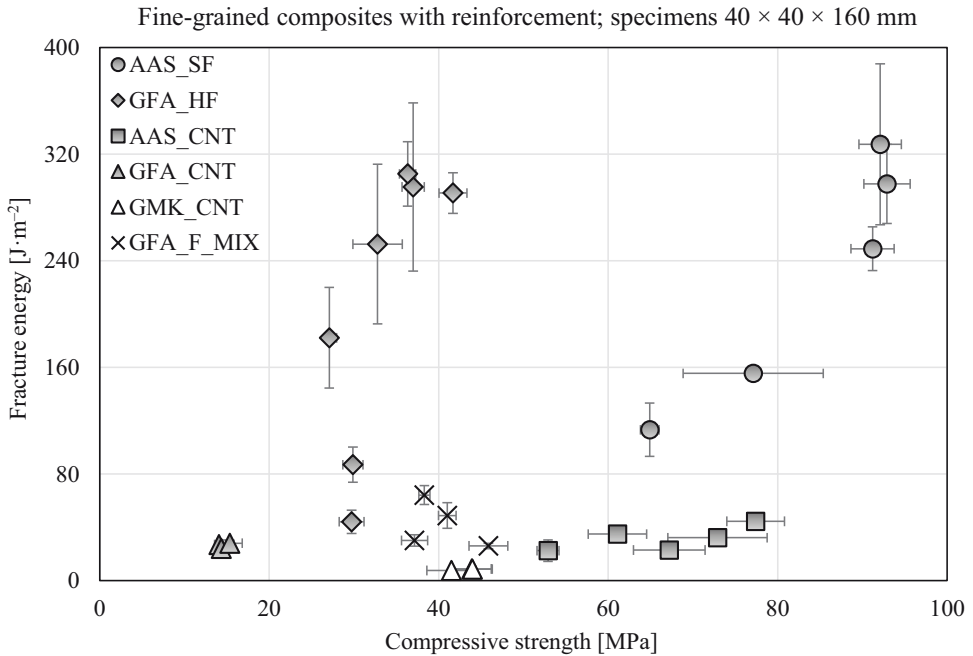


Figure 18. The specific fracture energy vs. compressive strength of selected investigated fine-grained composites with different reinforcement

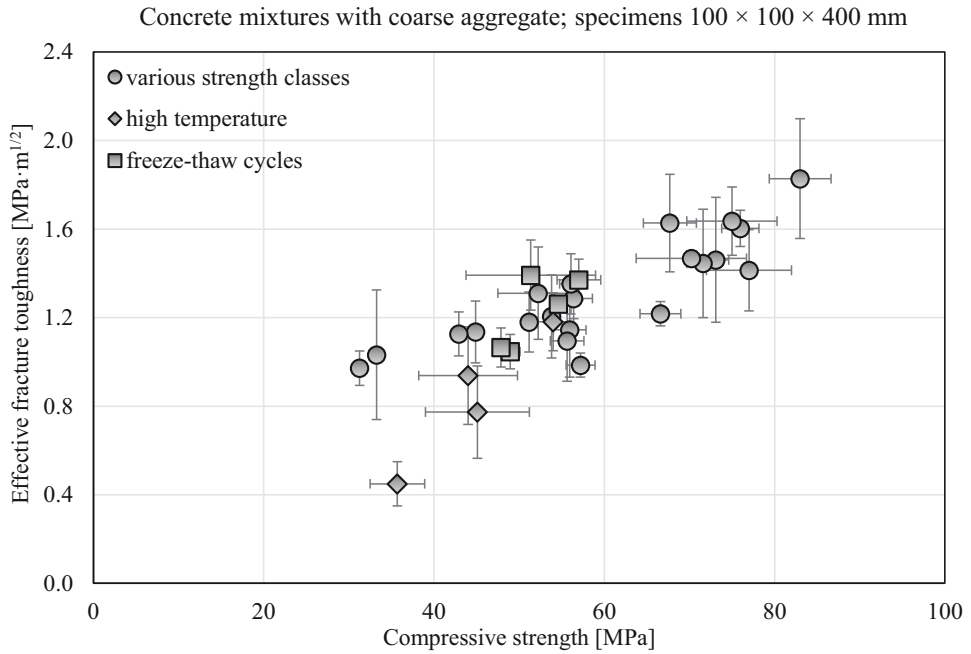


Figure 19. The effective fracture toughness vs. compressive strength of selected investigated concrete mixtures with coarse aggregate

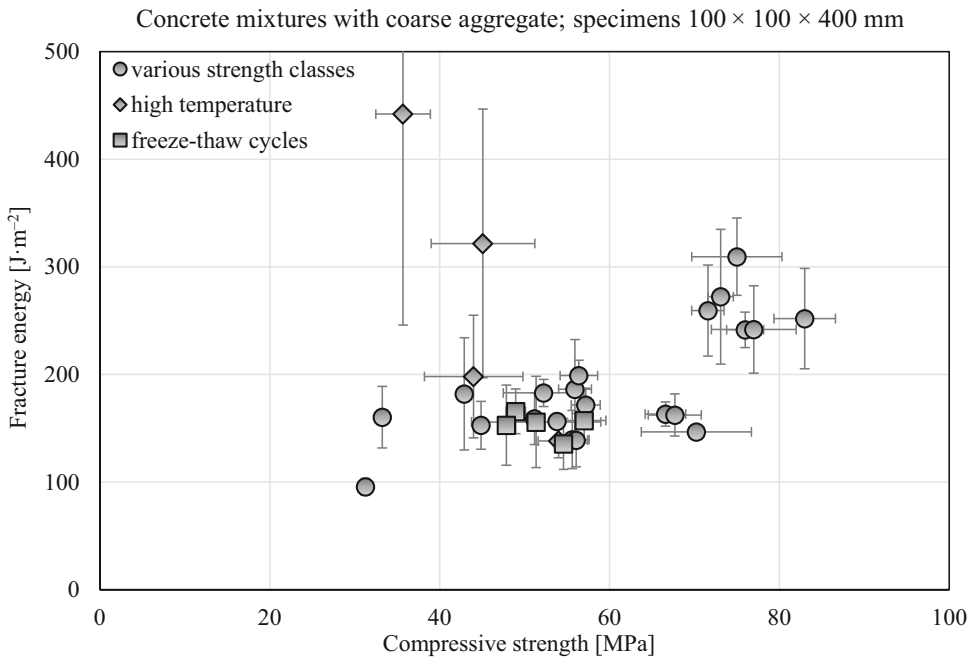


Figure 20. The specific fracture energy vs. compressive strength of selected investigated concrete mixtures with coarse aggregate

6 CONCLUDING REMARKS

The habilitation thesis summarizes the results and knowledge obtained by solving many partial tasks within the framework of research projects solved at the FCE, BUT in which the author has been involved since 2010. The main emphasis is put on the experimental determination of mechanical fracture and fatigue characteristics of various types of commonly used but also newly developed building composites with the brittle matrix.

The effective solution of comprehensive research tasks requires the cooperation of experts from various scientific fields. Therefore, the author of this thesis has had the opportunity to cooperate with experts from different institutes of the FCE, BUT and also colleagues from foreign universities since the beginning of her research career. This led to the author's engagement in the characterization of fracture behaviour of a whole range of different types of quasi-brittle materials: from mortars/fine-grained composites (lime (L) with different admixtures such as brick powder, metakaolin, bentonite, metaclay [64]; cement (C) with the admixture of slag, fly ash, metakaolin, brick powder, glass powder, zeolite [65–69]; alkali activated slag (AAS) with different composition [70, 71] and also reinforcement, e.g. carbon nanotubes (CNT) [71] and steel micro fibres (SF) [72]; alkali activated brick powder (AABP) [73]; fly ash (GFA) and metakaolin (GMK) based geopolymers with the admixture of CNT [74, 75]) and different types of fibres, e.g. hemp fibres (HF) [76]) to plenty of types of concrete such as plain concrete of different composition (water/cement ratio, with/without superplasticizer [77–79]); concrete with fibres (different types/length/volume of fibres [80, 81]); and composites based on AABs [82, 83]. Also, the fatigue parameters of different types of quasi-brittle materials were investigated [63, 83–85].

Mechanical fracture parameters are primarily obtained through the direct evaluation of fracture test data via the EFM [4] and 2K model [47] and the work-of-fracture method recommended by RILEM [6]. In addition, selected experimental data are used to determination of mechanical fracture parameters indirectly – based on a combination of fracture testing and inverse analysis. The fracture response recorded from the 3PB test of specimens made of selected fine-grained composites is used for verification of the proposed hybrid artificial neural network-based identification system [50, 70, 86]. The parameters which can be obtained from the inverse analysis are important, as they can be used to quantify structural resistance against crack initiation and propagation, as well as to compare studied or developed composites. They can also be employed for the definition of material models for the deterministic or stochastic simulation of the quasi-brittle/ductile response of composites/members using a stochastic finite element method (FEM) model based on non-linear fracture mechanics principles.

The mechanical fracture parameters help us to understand the relation between the macroscopic response of the specimen and its microstructural evolution during cracking of course considering size-effect [3]. This is crucial in the design and modelling of newly developing composites, as well as in the comparison of properties of commonly used and newly develop quasi-brittle composites. These parameters can be beneficial also in the assessment of internal damage of quasi-brittle materials caused by temperature changes. The alternate of the positive and negative temperatures (freeze-thaw cycles) is considered one of the most destructive processes which influence the durability of the structures substantially. As well high temperatures acting on quasi-brittle materials cause a wide range of physical and chemical processes, which result in changes in the structure of composites and thus affect the mechanical properties. The mechanical fracture parameters bring more complex information about material damage caused by low [87, 88] and high temperatures [89, 90] than standardized methods. Nevertheless, in many cases, the attention is still focused on the maximum strength of the material rather than analyzing the properties associated with resistance to crack formation and propagation.

REFERENCES

- [1] Červenka, V., Jendele, L., Červenka, J. *ATENA Program documentation – Part 1: theory*. Červenka Consulting: Prague, 2016.
- [2] Frantík, P. *FyDiK application*, 2015. <http://fydik.kitnarf.cz/>
- [3] Bažant, Z.P., Planas, J. *Fracture and Size Effect in Concrete and other Quasibrittle Materials*. CRC Press: Boca Raton, 1998, 640 p.
- [4] Karihaloo, B.L. *Fracture mechanics and structural concrete*. Longman Scientific & Technical: Harlow, Essex, England, 1995, 330 p.
- [5] Shah, S.P., Swartz, S.E., Ouyang, Ch. *Fracture mechanics of structural concrete: applications of fracture mechanics to concrete, rock, and other quasi-brittle materials*, 1st ed.; John Wiley & Sons, Inc.: New York, 1995, 592 p.
- [6] RILEM TC – 50 FMC (Recommendation). Determination of the fracture energy of mortar and concrete by means of three-point bend tests on notched beams. *Materials & Structures*. 1985, Vol. 18(4), pp. 287–290. <https://doi.org/10.1007/BF02472918>
- [7] RILEM TC– 89 FMT (Recommendation). Size-effect method for determining fracture energy and process zone size of concrete. *Materials & Structures*. 1990, Vol. 23, pp. 461–465.
- [8] Frantík, P. *CheCyId application*, 2017. <http://checyid.kitnarf.cz>
- [9] Novák, D., Lehký, D. ANN inverse analysis based on stochastic small-sample training set simulation. *Engineering Applications of Artificial Intelligence*. 2006, Vol. 19(7), pp. 731–740. <https://doi.org/10.1016/j.engappai.2006.05.003>
- [10] Lehký, D., Novák, D., Keršner, Z. FraMePID-3PB software for material parameter identification using fracture tests and inverse analysis. *Advances in Engineering Software*. 2014, Vol. 72, pp. 147–154. <https://doi.org/10.1016/j.advengsoft.2013.10.001>
- [11] Brühwiler, E., Wittmann, F.H. The wedge splitting test, a new method of performing stable fracture mechanics tests. *Engineering Fracture Mechanics*. 1990, Vol. 35(1–3), pp. 117–125. [https://doi.org/10.1016/0013-7944\(90\)90189-N](https://doi.org/10.1016/0013-7944(90)90189-N)
- [12] Tschegg, E.K. New equipments for fracture tests on concrete. *Materials Testing*. 1991, Vol. 33, pp. 338–342.
- [13] Lee, M.K., Barr, B.I.G. An overview of the fatigue behavior of plain and fibre reinforced concrete. *Cement and Concrete Composites*. 2004, Vol. 26 (4), pp. 299–305. [https://doi.org/10.1016/S0958-9465\(02\)00139-7](https://doi.org/10.1016/S0958-9465(02)00139-7)
- [14] Pyl, D., Červenka, J., Pukl, R. Material model for finite element modelling of fatigue crack growth in concrete. *Procedia Engineering*. 2010, Vol. 2 (1), pp. 203–212. <https://doi.org/10.1016/j.proeng.2010.03.022>
- [15] Toumi, A., Bascoul, A., Turatsinze, A. Modeling of fatigue crack growth in concrete subjected to mode I crack opening. In *Proc. of the 4th Int. Conf. on Fracture Mechanics of Concrete Structures*, de Borst, R. et al, eds. CRC Press: United Kingdom, 2001, pp. 637–640
- [16] Darweesh, H.H.M. Mortar Composites Based on Industrial Wastes. *International Journal of Materials Lifetime*. 2017, Vol. 3, No. 1, pp. 1–8. doi: 10.12691/ijml-3-1-1
- [17] Keun-Hyeok, Y., Yeon-Back, J., Myung-Sug, C., Sung-Ho, T. Effect of supplementary cementitious materials on reduction of CO2 emissions from concrete. *Journal of Cleaner Production*. 2015, Vol. 103, pp. 774–783. <https://doi.org/10.1016/j.jclepro.2014.03.018>
- [18] Keun-Hyeok, Y., Jin-Kyu, S., Keum-Il, S. Assessment of CO2 reduction of alkali-activated concrete. *Journal of Cleaner Production*. 2013, Vol. 39, pp. 265–272. <https://doi.org/10.1016/j.jclepro.2012.08.001>

- [19] McLellan, B.C., Williams, R.P., Lay, J., van Riessen, A., Corder, G.D. Costs and carbon emissions for geopolymer pastes in comparison to ordinary Portland cement. *Journal of Cleaner Production*. 2011, Vol. 19(10), pp. 1080–1090. <https://doi.org/10.1016/j.jclepro.2011.02.010>
- [20] Chen, W., Jin, R., Xu, Y., Wanatowski, D., Li, B., Yan, L., Pan, Z., Yang, Y. Adopting recycled aggregates as sustainable construction materials: A review of the scientific literature. *Construction and Building Materials*. 2019, Vol. 218, pp. 483–496. <https://doi.org/10.1016/j.conbuildmat.2019.05.130>
- [21] Rodrigues, F., Carvalho, M.T., Evangelista, L., de Brito, J. Physical–chemical and mineralogical characterization of fine aggregates from construction and demolition waste recycling plants. *Journal of Cleaner Production*. 2013, Vol. 52, pp. 438–445. <https://doi.org/10.1016/j.jclepro.2013.02.023>
- [22] Tošić, N. Marinković, S. Dašić, T. Stanić, M. Multicriteria optimization of natural and recycled aggregate concrete for structural use. *Journal of Cleaner Production*. 2015, Vol. 87, pp. 766–776. <https://doi.org/10.1016/j.jclepro.2014.10.070>
- [23] Sharma, N.K., Kumar, P., Kumar, S., Thomas, B.S., Gupta, R.C. Properties of concrete containing polished granite waste as partial substitution of coarse aggregate. *Construction and Building Materials*. 2017, Vol. 151, pp. 158–163. <https://doi.org/10.1016/j.conbuildmat.2017.06.081>
- [24] Anderson, D.J., Smith, S.T., Au, F.T.K. Mechanical properties of concrete utilizing waste ceramic as coarse aggregate. *Construction and Building Materials*. 2016, Vol. 117, pp. 20–28. <https://doi.org/10.1016/j.conbuildmat.2016.04.153>
- [25] Johnston, C.D. *Fiber-reinforced Cements and Concretes*. Taylor & Francis Group: London, 2010, 261p.
- [26] Smarzewski, P. Influence of basalt-polypropylene fibres on fracture properties of high performance concrete. *Composite Structures*. 2019, Vol. 209, pp. 23–33. <https://doi.org/10.1016/j.compstruct.2018.10.070>
- [27] Kizilkanat, A.B., Kabay, N., Akyüncü, V., Chowdhury, S., Akça, A.H. Mechanical properties and fracture behavior of basalt and glass fiber reinforced concrete: An experimental study. *Construction and Building Materials*. 2015, Vol. 100, pp. 218–224. <https://doi.org/10.1016/j.conbuildmat.2015.10.006>
- [28] Zhou, X., SAlni, H., Kastiukas, G. Engineering Properties of Treated Natural Hemp Fiber-Reinforced Concrete. *Frontiers in Building Environment*. 2017, Vol. 3, Article 33. <https://doi.org/10.3389/fbuil.2017.00033>
- [29] Zanichelli, A., Carpinteri, A., Fortese, G., Ronchei, C., Scorza, D., Vantadori, S. Contribution of date-palm fibres reinforcement to mortar fracture toughness. *Procedia Structural Integrity*. 2018, Vol. 13, pp. 542–547. <https://doi.org/10.1016/j.prostr.2018.12.089>
- [30] Tattersall, H.G., Tappin, G. The work of fracture and its measurement in metals, ceramics and other materials. *Journal of Materials Science*. 1966, Vol. 1, pp. 296–301. doi: 10.1007/BF00550177
- [31] Ouchterlony, F. Suggested methods for determining the fracture 2 toughness of rocks. *International Journal of Rock Mechanics and Mining Sciences*. 1988, Vol. 25, Iss. 2, pp. 71–96.
- [32] Šimonová, H., Daněk, P., Frantík, P., Keršner, Z., Veselý, V. Tentative characterization of old structural concrete through mechanical fracture parameters. *Procedia Engineering: Structural and Physical Aspects of Construction Engineering*. 2017, Vol. 109, pp. 414–418. doi: 10.1016/j.proeng.2017.05.357

- [33] Kucharczyková, B., Šimonová, H., Kocáb, D., Topolář, L. Advanced Evaluation of the Freeze–Thaw Damage of Concrete Based on the Fracture Tests. *Materials*. 2021, Vol. 14, Article No. 6378. doi: <https://doi.org/10.3390/ma14216378>
- [34] Merta, I., Tschegg, E.K. Fracture energy of natural fibre reinforced concrete. *Construction and Building Materials*. 2013, Vol. 40, pp. 991–997. <https://doi.org/10.1016/j.conbuildmat.2012.11.060>
- [35] Lehký, D., Kucharczyková, B., Šimonová, H., Daněk, P. Comprehensive fracture tests of concrete for the determination of mechanical fracture parameters. *Structural Concrete*. 2022, Vol. 23, Iss. 1, pp. 505–520. ISSN 1464-4177. <https://doi.org/10.1002/suco.202000496>
- [36] Irwin, G.R. Analysis of Stress and Strains Near the End of a Crack Traversing the Plate. *Journal of Applied Mechanics*. 1957, Vol. 24, pp. 361–364.
- [37] Kuruppu, M.D., Chong, K.P. Fracture toughness testing of brittle materials using semi-circular bend (SCB) specimen. *Engineering Fracture Mechanics*. 2012, Vol. 91, pp. 133–150. <https://doi.org/10.1016/j.engfracmech.2012.01.013>
- [38] Razmi, A., Mirsayar, M.M. On the mixed mode I/II fracture properties of jute fiber-reinforced concrete. *Construction and Building Materials*. 2017, Vol. 148, pp. 512–520. <https://doi.org/10.1016/j.conbuildmat.2017.05.034>
- [39] Erarslan, N. Analysing mixed mode (I–II) fracturing of concrete discs including chevron and straight-through notch cracks. *International Journal of Solids and Structures*. 2019, Vol. 167, pp. 79–92. <https://doi.org/10.1016/j.ijsolstr.2019.03.005>
- [40] Xing, Y., Huang, B., Ning, E., Zhao, L., Jin, F. Quasi-Static Loading Rate Effects on Fracture Process Zone Development of Mixed-Mode (I-II) Fractures in Rock-Like Materials. *Engineering Fracture Mechanics*. 2020, Vol. 240, Article No. 107365. <https://doi.org/10.1016/j.engfracmech.2020.107365>
- [41] Alanazi, N., Susmel, L. Estimating static/dynamic strength of notched unreinforced concrete under mixed mode I/II loading. *Engineering Fracture Mechanics*. 2020, Vol. 240, Article No. 107329. <https://doi.org/10.1016/j.engfracmech.2020.107329>
- [42] Ruiz, G., de la Rosa, A., Almeida, L.C., Poveda, E., Zhang, X.X., Tarifa, M., Wu, Z.M., Yu, R.C. Dynamic mixed-mode fracture in SCC reinforced with steel fibers: an experimental study. *International Journal of Impact Engineering*. 2019, Vol. 129, pp. 101–111. <https://doi.org/10.1016/j.ijimpeng.2019.03.003>
- [43] Aliha, M.R.M., Mousavi, S.S., Ghoreishi, S.M.N. Fracture load prediction under mixed mode I+II using a stress based method for brittle materials tested with the asymmetric four-point bend specimen. *Theoretical and Applied Fracture Mechanics*. 2019, Vol. 103, Article No. 102249. <https://doi.org/10.1016/j.tafmec.2019.102249>
- [44] Malíková, L., Miarka, P., Kucharczyková, B., Šimonová, H. Williams expansion utilized for assessment of crack behaviour under mixed-mode loading in alkali-activated fine-grained composite. *Fatigue & Fracture of Engineering Materials & Structures*. 2021, Vol. 44, Iss. 5, pp. 1151–1161. <https://doi.org/10.1111/ffe.13418>
- [45] Frantík, P., Mašek, J. *GTDiPS software*, 2015. Available online: <http://gtdips.kitnarf.cz/>
- [46] Stibor, M. *Fracture Parameters of Quasi-Brittle Materials and Their Determination* (in Czech). Dissertation thesis, Brno University of Technology, Brno, 2004.
- [47] Kumar, S., Barai, S.V. *Concrete Fracture Models and Applications*. Springer: Berlin, 2011, 262 p.
- [48] Hordijk, D.A. *Local approach to fatigue of concrete*. PhD Thesis, Technische Universiteit Delft, Delft, Netherlands, 1991.

- [49] Lehký, D., Keršner, Z., Novák, D. FraMePID-3PB software for material parameter identification using fracture tests and inverse analysis. *Advances in Engineering Software*. 2014, Vol. 72, pp. 147–154. <https://doi.org/10.1016/j.advengsoft.2013.10.001>
- [50] Lehký, D., Lipowczan, M., Šimonová, H., Keršner, Z. 2021. A hybrid artificial neural network-based identification system for fine-grained composites. *Computers and Concrete*. 2021, Vol. 28, Iss. 4, pp. 369–378. doi: <https://doi.org/10.12989/cac.2021.28.4.369>
- [51] Jenq, Y.S., Shah, S.P. Two parameter fracture model for concrete. *Journal of Engineering Mechanics*. 1985, Vol. 111, Iss. 10, pp. 1227–1241. [https://doi.org/10.1061/\(ASCE\)0733-9399\(1985\)111:10\(1227\)](https://doi.org/10.1061/(ASCE)0733-9399(1985)111:10(1227))
- [52] Xu, S., Reinhardt, H.W. Determination of double-K criterion for crack propagation in quasibrittle fracture, Part II: Analytical evaluating and practical measuring methods for three-point bending notched beams. *International Journal of Fracture*. 1999, Vol. 98, Iss. 2, pp. 151–177. <https://doi.org/10.1023/a:1018740728458>
- [53] Miura, T., Sato, K., Nakamura, H. Influence of primary cracks on static and fatigue compressive behavior of concrete under water. *Construction and Building Materials*. 2021, Vol. 305, Article No. 124755. <https://doi.org/10.1016/j.conbuildmat.2021.124755>
- [54] Zhang J., Stang H., Li V.C. Experimental study on crack bridging in FRC under uniaxial fatigue tension. *Journal of Materials in Civil Engineering*. 2000, Vol. 12, Iss. 1, pp. 66–73. [https://doi.org/10.1061/\(ASCE\)0899-1561\(2000\)12:1\(66\)](https://doi.org/10.1061/(ASCE)0899-1561(2000)12:1(66))
- [55] Saini, B.S., Singh, S.P. Flexural fatigue life analysis of self compacting concrete containing 100% coarse recycled concrete aggregates. *Construction and Building Materials*. 2020, Vol. 253, Article No. 119176. <https://doi.org/10.1016/j.conbuildmat.2020.119176>
- [56] Zhang, J., Li, V.C., Stang, H. Size effect on fatigue in bending of concrete. *Journal of Materials in Civil Engineering*. 2001, Vol. 13, Iss. 6, pp. 446–453. [https://doi.org/10.1061/\(ASCE\)0899-1561\(2001\)13:6\(446\)](https://doi.org/10.1061/(ASCE)0899-1561(2001)13:6(446))
- [57] Kirane, K., Bažant, Z.P. Size effect in Paris law and fatigue lifetimes for quasibrittle materials: Modified theory, experiments and micro-modeling. *International Journal of Fatigue*. 2016, Vol. 83, pp. 209–220. <https://doi.org/10.1016/j.ijfatigue.2015.10.015>
- [58] Miarka, P., Seitl, S., Bílek, V., Cifuentes, H. Assessment of fatigue resistance of concrete: S-N curves to the Paris' law curves. *Construction and Building Materials*. 2021, Vol. 341, Article No. 127811. <https://doi.org/10.1016/j.conbuildmat.2022.127811>
- [59] RILEM Committee 36-RD. Long term random dynamic loading of concrete structures, *Materials & Structures*. 1984, Vol. 17, Iss. 97, pp. 1–28.
- [60] Věchet, S., Král, P. *Únava materiálu: Únava materiálu úvod*. In NoM I – 6, *Únava materiálu*, 2007. p. 1–9.
- [61] Weibull, W. *Fatigue testing and analysis of results*. Pergamon press: Oxford, 1961.
- [62] Šimonová, H., Havlíková, I., Keršner, Z., Seitl, S. Statistical evaluation of fatigue tests of plain C30/37 and C45/55 class concrete specimens. In: *Proc. of 8th Int. Conf. on Fracture Mechanics of Concrete and Concrete Structures, FraMCos-8*. Barcelona: International Center for Numerical Methods in Engineering (CIMNE), 2013, pp. 862–867.
- [63] Abdel-Jawad, Y.A. The maturity method: Modifications to improve estimation of concrete strength at later ages. *Construction and Building Materials*. 2006, Vol. 20, pp. 893–900. <https://doi.org/10.1016/j.conbuildmat.2005.06.022>
- [64] Šimonová, H., Havlíková, I., Navrátilová, E., Schmid, P., Rovnaníková, P., Keršner, Z. Effect of Admixture Dosage and Specimens Age on Mechanical Fracture Parameters of Lime Mortars Enhanced by Burnt Clays. *Advanced Materials Research: Ecology and New Building Materials and Products*. 2014, Vol. 1000, pp. 356–359. www.scientific.net/AMR.1000.356

- [65] Bílek, V. Jr., Topolář, L., Šimonová, H., Kucharczyková, B., Havlíková, I., Pazdera, L., KERŠNER, Z. Pilot Study of the Effect of Admixtures in Fine-grained Cement-based Composites on Volume Changes and Fracture Parameters. *Advanced Materials Research: Structural and Physical Aspects of Civil Engineering*. 2014, Vol. 969, pp. 294–297.
- [66] Rovnaníková, P., Šimonová, H., Schmid, P., Zahálková, J., Bayer, P., Havlíková, I., Keršner, Z. Mechanical Fracture properties of Cement Mortars with Diatomite in relation to their Microstructure. *Advanced Materials Research: Ecological and New Building Materials and Products*. 2015, Vol. 1124, pp. 57–62. doi: 10.4028/www.scientific.net/AMR.1124.57
- [67] Šimonová, H., Zahálková, J., Rovnaníková, P., Bayer, P., Keršner, Z., Schmid, P. Mechanical Fracture Parameters of Cement Based Mortars with Waste Glass Powder. *Procedia Engineering: Structural and Physical Aspects of Construction Engineering*. 2017, Vol. 109, pp. 86–91. ISSN 1877-7058. doi: 10.1016/j.proeng.2017.05.311
- [68] Šimonová, H., Schmid, P., Keršner, Z., Rovnaníková, P. Mechanical Fracture Parameters of Fine-grain Concretes with Zeolite: Effect of Composition and Origin of Cements. *Advanced Materials Research: Ecology and New Building Materials and Products*. 2014, Vol. 1000, pp. 330–333. www.scientific.net/AMR.1000.330.
- [69] Havlikova, I., Bilek, V. Jr., Topolar, L., Simonova, H., Schmid, P., Kersner, Z. Modified Cement-based Mortars: Crack Initiation and Volume Changes. *Materiali in technologie/Materials and technology*. 2015, Vol. 49, Issue 4, pp. 557–561
- [70] Šimonová, H., Kucharczyková, B., Bílek, V., Malíková, L., Miarka, P., Lipowczan, M. Mechanical Fracture and Fatigue Characteristics of Fine-Grained Composite Based on Sodium Hydroxide-Activated Slag Cured under High Relative Humidity. *Applied Sciences*. 2021, vol. 11, Article No. 259. <https://doi.org/10.3390/app11010259>
- [71] Rovnaník, P., Šimonová, H., Topoláč, L., Bayer, P., Schmid, P., Keršner, Z. Carbon nanotube reinforced alkali-activated slag mortars. *Construction and Building Materials*. 2016, Vol. 119, pp. 223–229. <http://dx.doi.org/10.1016/j.conbuildmat.2016.05.051>
- [72] Šimonová, H., Frantík, P., Keršner, Z., Schmid, P., Rovnaník, P. Components of the fracture response of alkali-activated slag composites with steel microfibers. *Applied Sciences*. 2019, Vol. 9, No. 9, Article No.1754. <https://doi.org/10.3390/app909175>
- [73] Šimonová, H., Lipowczan, M., Rozsypalová, I., Daněk, P., Lehký, D., Rovnaníková, P., Keršner, Z. Fracture parameters of alkali-activated aluminosilicate composites with ceramic precursor: durability aspects. *Procedia Structural Integrity*. 2021, Vol. 33, pp. 207–214. doi: 10.1016/j.prostr.2021.10.025
- [74] Rovnaník, P., Šimonová, H., Topolář, L., Schmid, P., Keršner, Z. Effect of carbon nanotubes on the mechanical fracture properties of fly ash geopolymer. *Procedia Engineering: Ecology and new building materials and products 2016*. Elsevier, 2016, Vol. 151, pp. 321–328. <http://dx.doi.org/10.1016/j.proeng.2016.07.360>
- [75] Šimonová, H., Topolář, L., Schmid, P., Keršner, Z., Rovnaník, P. Effect of Carbon Nanotubes in Metakaolin-based Geopolymer Mortars on Fracture Toughness Parameters and Acoustic Emission Signals. *Brittle Matrix Composites II*. Warsaw: ZTUREK Research-Scientific Institute and Institute of Fundamental Technological Research, 2015, pp. 261–267.
- [76] Simonova, H., Kucharczykova, B., Topolar, L., Kersner, Z., Merta, I., Dragas, J., Ignjatovic, I., Komljenovic, M., Nikolic, V. Crack initiation of selected geopolymer mortar with hemp fibres. *Procedia Structural Integrity: ECF22 – Loading and Environmental effects on Structural Integrity*. 2018, Vol. 13, pp. 578–583. <https://doi.org/10.1016/j.prostr.2018.12.095>

- [77] Šimonová, H., Daněk, P., Frantík, P., Keršner, Z., Veselý, V. Tentative characterization of old structural concrete through mechanical fracture parameters. *Procedia Engineering: Structural and Physical Aspects of Construction Engineering*. 2017, Vol. 109, pp. 414–418. doi: 10.1016/j.proeng.2017.05.357
- [78] Lehký, D., Kucharczyková, B., Šimonová, H., Daněk, P. Comprehensive fracture tests of concrete for the determination of mechanical fracture parameters. *Structural Concrete*. 2022, Vol. 23, Iss. 1, pp. 505–520. <https://doi.org/10.1002/suco.202000496>
- [79] Šimonová, H., Havlíková, I., Daněk, P., Keršner, Z., Vymazal, T. The Effect of a Superplasticizer Admixture on the Mechanical Fracture Parameters of Concrete. *Materiali in technologie/Materials and technology*. 2015, Vol. 49, Issue 3, pp. 417–421.
- [80] Havlíková, I., Šimonová, H., Pail, T., Navrátilová, E., Majtánová, R. V., Keršner, Z. Effect of Softening Function Type in the Double-K Fracture Model for the Evaluation of Fracture Tests on Concrete Specimens with and without polypropylene Fibres. *Proc. of Int. Conf. on ENGINEERING MECHANICS 2013*. Praha: Institute of Thermomechanics, Academy of Sciences of the Czech Republic, v. v. i., 2013, pp. 152–159.
- [81] Lehký, D., Řoutil, L., Keršner, Z., Novák, D., Šimonová, H., Havlíková, I., Schmid, P. Experimental determination of mechanical fracture parameters of steel fiber reinforced concrete for probabilistic life-cycle assessment. *Concrete – Innovation and Design, fib Symposium Proceedings*. Copenhagen, Denmark: Danish Concrete Society, 2015, pp. 1–8.
- [82] Šimonová, H., Kucharczyková, B., Topolář, L., Bílek, V., Jr., Keršner, Z. Fracture properties of concrete specimens made from alkali activated binders. *IOP Conf. Series: Materials Science and Engineering*. 2017, Vol. 236, 012068. doi:10.1088/1757-899X/236/1/012068
- [83] Seitl, S., Bílek, V., Šimonová, H., Keršner, Z. Mechanical and fatigue parameters of two types of alkali-activated concrete. *Key Engineering Materials: Advances in Fracture and Damage Mechanics XIV*. 2016, Vol. 665, pp. 129–132. doi: 10.4028/www.scientific.net/KEM.665.129
- [84] Seitl, S., Miarka, P., Šimonová, H., Frantík, P., Keršner, Z., Domski, J., Katzer, J. Change of Fatigue and Mechanical Fracture Properties of a Cement Composite due to Partial Replacement of Aggregate by Red Ceramic Waste. *Periodica Polytechnica Civil Engineering*. 2019, Vol. 63, No. 1, pp. 152–159. <https://doi.org/10.3311/PPci.12450>
- [85] Šimonová, H., Veselý, V., Keršner, Z., Culík, L., Mosler, T., Bílek, V. Influence of the Age and Level of Concrete fatigue on Prestressed Railway Sleepers Response: Parametric Study and Experiment. *Advanced Materials Research: Structural and Physical Aspects of Civil Engineering*. 2014, Vol. 969, pp. 218–221.
- [86] Lipowczan, M., Lehký, D., Šimonová, H., Kucharczyková, B., Keršner, Z. Identification of mechanical fracture parameters of fine-grained brittle matrix composites. *Proceedings of the 2021 session of the 13th fib International PhD Symposium in Civil Engineering*. Switzerland: International Federation for Structural Concrete, 2021, pp. 10–17.
- [87] Kucharczyková, B., Šimonová, H., Kocáb, D., Topolář, L. Advanced Evaluation of the Freeze–Thaw Damage of Concrete Based on the Fracture Tests. *Materials*. 2021, Vol. 14, Article No. 6378. doi: <https://doi.org/10.3390/ma14216378>
- [88] Kucharczyková, B., Šimonová, H., Kocáb, D., Fernandes, G. Non-traditional Approach to the Evaluation of the Freeze-thaw Resistance of Concrete based on the Fracture Tests. *MATEC Web of Conferences, MATBUD'2020 – Scientific-Technical Conference: E-mobility, Sustainable Materials and Technologies*. 2020, Vol. 322, Article No. 01015. doi: <https://doi.org/10.1051/mateconf/202032201015>

- [89] Šimonová, H., Rozsypalová, I., Rovnaníková, P., Daněk, P., Keršner, Z. Thermal Analysis of Concrete from Panels Subjected to Fire Experiments. *Solid State Phenomena: 24th Concrete Days 2017*. 2018, Vol. 272, pp. 47–52. doi: 10.4028/www.scientific.net/SPP.272.47
- [90] Šimonová, H., Trčka, T., Bejček, M., Rozsypalová, I., Daněk, P., Keršner, Z. Detailed Determination of Mechanical Fracture Parameters of Concrete after Fire Experiments. *Solid State Phenomena: 24th Concrete Days 2017*. 2018, Vol. 272, pp. 220–225. doi: 10.4028/www.scientific.net/SPP.272.220

ABSTRACT

The habilitation thesis summarizes the results and knowledge obtained by solving many partial tasks within the framework of research projects solved at the Faculty of Civil Engineering, the Brno University of Technology in which the author has been involved. The main emphasis is put on the experimental determination of mechanical fracture and fatigue characteristics of various types of commonly used but also newly developed building composites with the brittle matrix. This habilitation thesis is constituted through a series of published articles on selected topics. To sum up, this thesis consists of nine journal papers and two conference proceeding papers.

ABSTRAKT

Předložená habilitační práce shrnuje výsledky a poznatky získané řešením celé řady dílčích úkolů v rámci výzkumných projektů řešených na Fakultě stavební Vysokého učení technického v Brně, do nichž byla autorka práce zapojena. Hlavní důraz je v práci kladen na vyhodnocení statických a únavových lomových experimentů těles z různých typů běžně používaných ale i nově vyvíjených kompozitů s křehkou maticí. Tato habilitační práce je tvořena sérií publikovaných článků na vybraná témata. V souhrnu se tato práce skládá z devíti článků publikovaných ve vědeckých časopisech a dvou příspěvků uveřejněných ve sbornících mezinárodních konferencí.